Model of the auxin response gene regulatory network

Ancient Trans-acting siRNAs Confer Robustness and Sensitivity onto the Auxin Response

Yevgeniy Plavskin[1,2], Akitomo Nagashima[3,4], Pierre-François Perroud[5,6], Mitsuyasu Hasebe[3,4], Ralph S. Quatrano[5], Gurinder S. Atwal[1], Marja C.P. Timmermans[1,7]

1. Watson School of Biological Sciences, Cold Spring Harbor Laboratory, Cold Spring Harbor, NY, USA
2. Present address: Department of Biology, NYU Center for Genomics and Systems Biology, New York, NY, USA
3. National Institute for Basic Biology, Okazaki, Japan
4. Exploratory Research for Advanced Technology, Japan Science and Technology Agency, Okazaki, Japan
5. Department of Biology, Washington University, St. Louis, MO, USA
6. Present address: Department of Cell Biology II, Philipps-Universität Marburg, Marburg, Germany
7. Center for Plant Molecular Biology, University of Tübingen, Tübingen, Germany

Overview

This note supplements the information presented in the main text of the paper regarding the ordinary differential equation (ODE)-based computational model of the auxin response GRN. Here, we provide a detailed explanation of the ODEs that make up the model. We derive a numerical solution for steady state GRN component levels for a given auxin signaling input level. We also describe the values used in this model for physical parameters of the auxin response GRN, and demonstrate that our findings regarding the effects of small RNA regulation on susceptibility and extrinsic noise amplification levels are robust across a wide range of parameter values. We further show that results are robust to changes in the properties of the extrinsic noise modeled, and hold true regardless of whether small RNA activity is modeled as promoting degradation or translational repression of target transcripts. Finally, we explore the effect of autoregulation by repressor ARF proteins on susceptibility and noise amplification.

Introduction to the thermodynamic GRN model

At the core of the ODEs describing the behavior of the auxin response GRN is a thermodynamic model of auxin-responsive gene (ARG) activation (**Equation S9**). This equation computes the equilibrium probability that an RNA polymerase molecule is bound to the ARG promoter. This probability is, in turn, directly proportional to promoter activation and ARG transcription levels. The statistical mechanical approach to calculating this probability, which we adopt here, is described in detail in Bintu *et al*. (2005a). In brief, all possible promoter states are enumerated, and the probability of RNA polymerase binding is determined by computing the ratio of the statistical weights of all *'active'* promoter states over the weights of all possible promoter states. These statistical weights are proportional to the concentrations of relevant promoter-binding molecules, e.g. activator or repressor transcription factors, as well as promoter binding constants and constants describing interaction strengths among transcription factors, which accounts for any cooperativity in binding (see **Equation S9** and **Table SM1**). In the numerator of the polymerase binding probability equation, all active promoter states are scaled by a constant denoting the strength of RNA polymerase recruitment by that state. Like all thermodynamic approaches, the model described in Bintu *et al*. (2005a), and employed both in this work and in the work of Vernoux *et al*. (2011), implicitly invokes an adiabatic approximation to cleanly decouple the fast timescale of intrinsic transcriptional noise from the longer developmental

timescales that occur on the order of hours, days, and weeks. This results in a dynamical gene network model that explicitly employs the powerful formalism of thermodynamics to predict averaged gene expression levels.

Summary of the ODE model

The ODE-based model used in this work is adapted from the model developed by Vernoux *et al*. (2011). However, the following key modifications are added to reflect the auxin response GRN defined for *Physcomitrella* (**Equations S6-S9**). This model includes explicit terms for repressor ARF proteins and transcripts, rather than a general 'repression' term, as well as feedback between the auxin response and repressor ARF levels. The explicit modeling of repressor ARF levels allows tasiARF activity to be modeled by altering repressor ARF transcript degradation or translation rates, and thus provides insights into the properties the ancient *TAS3* tasiRNA pathway confers on the auxin response GRN.

Although not formerly demonstrated, a commonly accepted paradigm for auxin-dependent gene regulation is that activator and repressor ARFs compete for binding to a common set of ARG promoters. This framework is in line with our experimental data showing that overexpression of repressor *ARFb* genes results in phenotypes resembling those of auxin-resistant mutants. Our model therefore considers an ARG promoter as being co-regulated by activator and repressor ARFs. The equations governing the behavior of the *Physcomitrella* auxin response GRN model are represented pictorially in **Figure SM1**. These equations are as follows: **Equations S1-S9**, with an explanation of each parameter and variable provided in **Table SM1**:

$$\frac{d[\mathrm{IA}]}{d\mathrm{t}} = \pi_{\mathrm{IA}} * [\mathrm{IA}_{\mathrm{TRANSCRIPT}}] + 2 * k'_{\mathrm{IX}} * [\mathrm{D}_{\mathrm{IA:IA}}] - 2 * k_{\mathrm{IX}} * [\mathrm{IA}]^2 + k'_{\mathrm{IX}} * [\mathrm{D}_{\mathrm{IA:A+}}] - \ldots \\ k_{\mathrm{IX}} * [\mathrm{IA}] * [\mathrm{A+}] + [\mathrm{D}_{\mathrm{IA:IA}}] * \gamma_{\mathrm{AUXIN}}(\mathrm{x}) - [\mathrm{IA}] * \gamma_{\mathrm{AUXIN}}(\mathrm{x}) \quad \text{(S1)}$$

$$\frac{d[\mathrm{A+}]}{d\mathrm{t}} = \pi_{\mathrm{A+}} + k'_{\mathrm{IX}} * [\mathrm{D}_{\mathrm{IA:A+}}] - k_{\mathrm{IX}} * [\mathrm{IA}] * [\mathrm{A+}] + [\mathrm{D}_{\mathrm{IA:A+}}] * \gamma_{\mathrm{AUXIN}}(\mathrm{x}) - [\mathrm{A+}] * \gamma_{\mathrm{A+}} \quad \text{(S2)}$$

$$\frac{d[\mathrm{D}_{\mathrm{IA:IA}}]}{d\mathrm{t}} = k_{\mathrm{IX}} * [\mathrm{IA}]^2 - [\mathrm{D}_{\mathrm{IA:IA}}] * (k'_{\mathrm{IX}} + \gamma_{\mathrm{IX}} + \gamma_{\mathrm{AUXIN}}(\mathrm{x})) \quad \text{(S3)}$$

$$\frac{d[\mathrm{D}_{\mathrm{IA:A+}}]}{d\mathrm{t}} = k_{\mathrm{IX}} * [\mathrm{IA}] * [\mathrm{A+}] - [\mathrm{D}_{\mathrm{IA:A+}}] * (k'_{\mathrm{IX}} + \gamma_{\mathrm{IX}} + \gamma_{\mathrm{AUXIN}}(\mathrm{x})) \quad \text{(S4)}$$

Vernoux *et al*. (2011) demonstrated that if the association between auxin co-receptors, auxin, and Aux/IAA proteins occurs on a faster timescale than ubiquitination of Aux/IAA proteins, then changes in auxin signaling input can be described in terms of changes to Aux/IAA protein degradation rates, and we have adopted this simplification in our model. γ_{AUXIN}, the auxin-dependent degradation rate of Aux/IAA protein, is described by:

$$\gamma_{AUXIN}(x) = \gamma_{MAX} * \gamma_{IA} * \frac{K_{AUXIN} * x}{1 + K_{AUXIN} * x} \quad \text{(S5)}$$

As stated above, unlike the earlier model (Vernoux et al., 2011), which used a general 'repression' term to account for the activity of repressor ARF proteins, this model incorporates an explicit term for repressor ARF proteins (A-), which are produced from ARF- transcript and participate in the regulation of auxin-responsive gene (ARG) transcription (**Equation S6**). Both γ_{A-}, the repressor ARF transcript degradation rate, and π_{A-}, the repressor ARF translation rate, can be adjusted to model different levels of tasiARF activity. When repressor ARF autoregulation is included in the model, ARF- transcript ($A-_{transcript}$), like Aux/IAA transcript ($IA_{transcript}$), becomes a product of ARG transcription.

As described in the *Introduction to the thermodynamic GRN model*, the transcription rate of ARGs is proportional to the probability of RNA polymerase binding (Bintu 2005a). To translate the probability of RNA polymerase binding (h) into transcription rate, a scaling parameter can be used. However, to produce a model that qualitatively predicts the behavior of the auxin response GRN with a minimum number of free parameters, we chose to not fit this. Instead, we extensively explore the effects of changing the promoter activation strength (see below), and used a scaling of 0.5 throughout the model to calculate the transcription rate of $IA_{transcript}$ and $A-_{transcript}$ (**Equations S7 and S8**).

$$\frac{d[A-]}{dt} = \pi_{A-} * [A-_{TRANSCRIPT}] - [A-] * \gamma_{A-} \quad \text{(S6)}$$

$$\frac{d[IA_{TRANSCRIPT}]}{dt} = -\gamma_{IA\ transcript} * [IA_{TRANSCRIPT}] + \frac{1}{2} h([A+],[IA],[A-],[D_{IA:A+}]) \quad \text{(S7)}$$

$$\frac{d[A-_{TRANSCRIPT}]}{dt} = -\gamma_{A-\ transcript} * [A-_{TRANSCRIPT}] + \frac{1}{2} h([A+],[IA],[A-],[D_{IA:A+}]) \quad \text{(S8)}$$

$$h\left(\left[\mathrm{A+}\right],\left[\mathrm{IA}\right],\left[\mathrm{A-}\right],\left[\mathrm{D_{IA:A+}}\right]\right)=\frac{1+\frac{f*\left[\mathrm{A+}\right]}{k'_{\mathrm{P}}}+\frac{f*f_{\mathrm{A}}*\omega_{\mathrm{A}}*\left[\mathrm{A+}\right]*\left[\mathrm{A+}\right]}{k'_{\mathrm{P}}*k'_{\mathrm{P}}}}{1+\frac{\left[\mathrm{A+}\right]}{k'_{\mathrm{P}}}+\frac{\omega_{\mathrm{A}}*\left[\mathrm{A+}\right]*\left[\mathrm{A+}\right]}{k'_{\mathrm{P}}*k'_{\mathrm{P}}}+\frac{\omega_{\mathrm{I}}*\left[\mathrm{A+}\right]*\left[\mathrm{IA}\right]}{K_{\mathrm{dIX}}k'_{\mathrm{P}}}+\frac{\omega_{\mathrm{D}}*\left[\mathrm{D_{IA:A+}}\right]}{k'_{\mathrm{P}}}+\frac{\left[\mathrm{A-}\right]}{k'_{\mathrm{P}}}} \quad \text{(S9)}$$

Table SM1: overview of model parameters and variables

Variable/ Parameter	Explanation	Value in model*	Values tested
[A+]	Concentration of activator ARF protein in the cell		
[A-]	Concentration of repressor ARF protein in the cell		
[$A\text{-}_{transcript}$]	Concentration of repressor ARF transcript in the cell		
[$D_{IA:A+}$]	Concentration of activator ARF-Aux/IAA protein heterodimer in the cell		
[$D_{IA:IA}$]	Concentration of Aux/IAA protein homodimer in the cell		
[IA]	Concentration of Aux/IAA protein in the cell		
[$IA_{transcript}$]	Concentration of Aux/IAA transcript in the cell		
f	Strength of enhancement in specific RNA polymerase recruitment due to single activator ARF binding promoter	10	1-100
f_A	Strength of enhancement in specific RNA polymerase recruitment due to two activator ARFs binding promoter	10	1-100
k_{IX}	Association rate of dimer-forming reaction between an Aux/IAA protein and either an Aux/IAA protein or an activator ARF protein	1	0.1-5
k'_{IX}	Dissociation rate of dimer-forming reaction between an Aux/IAA protein and either an Aux/IAA protein or an activator ARF protein	10	1-100
k'_P	The dissociation rate of the ARF-promoter binding reaction	100	10-1000
K_{dIX}	Dissociation constant of Aux/IAA homo- or heterodimerization reaction ($K_{dIX} = k'_{IX} / k_{IX}$)	10	2-100
K_{AUXIN}	Affinity of auxin to its coreceptors	1	0.1-5
x	Auxin signaling input level	3.11	0.5-20
γ_{A+}	Degradation rate of activator ARF protein	0.003 (4 hours)	0.0005-0.5 (1.4 min – 23 hours)
γ_{A-}	Degradation rate of repressor ARF protein	0.003 (4 hours)	0.0005-0.5 (1.4 min – 23 hours)
γ_{AUXIN}	Degradation rate of Aux/IAA protein, which is a function of auxin signaling input level, x.	-	-

Table SM1 (continued)

Variable/ Parameter	Explanation	Value in model*	Values tested
γ_{MAX}	Largest fold increase in Aux/IAA degradation rate that can be induced by auxin binding	10	2-100
γ_{IA}	Degradation rate of Aux/IAA monomer in the absence of auxin	0.05 (14 min)	0.0005-0.5 (1.4 min - 23 hours)
γ_{IX}	Non-auxin dependent degradation rate of Aux/IAA homo- and heterodimers	0.003 (4 hours)	0.0005-0.5 (1.4 min - 23 hours)
$\gamma_{IA\ transcript}$	Degradation rate of Aux/IAA transcript	0.007 (100 min)	0.0005-0.5 (1.4 min - 23 hours)
π_{A+}	Production rate of activator ARF	1	0.1-5
π_{A-}	Translation rate of repressor ARF, tunable by sRNAs	1	10^{-3}-10^{4}
π_{IA}	Translation rate of Aux/IAA	1	0.1-5
ω_{A+}	Cooperativity effect of the dimerization of two activator ARFs on the promoter	10	1-100
ω_{I}	Cooperativity effect of the dimerization of Aux/IAA with an activator ARF on the promoter	10	1-100
ω_{D}	Cooperativity effect of binding of a Aux/IAA-activator ARF dimer to the promoter	10	1-100

* The parameter values listed are used in the model except where otherwise indicated. All time values are in minutes or minutes^{-1}. Where appropriate, half-life times are indicated in parentheses.

Selection of parameter values

Quantitative data on gene expression parameters in *Physcomitrella* is still limited. The selection of parameter values is therefore primarily based on Vernoux *et al*. (2011). However, it is important to note that the model presented here serves as a formal framework to explore effects of specific perturbations on signaling properties, i.e. susceptibility and noise amplification, of the auxin response network. As discussed below and in the main text, these primarily qualitative observations are robust to a wide range of parameter value choices, often across more than 2 orders of magnitude.

A detailed justification of value choices for most parameters can be found in Vernoux *et al*. (2011). Briefly, the values of γ_{A+} and γ_{A-} are based on the half-life of AtARF1 (Salmon et al., 2008); $\gamma_{IA\ transcript}$ is based on the average half-life of *AtAux/IAA* transcripts (Narsai et al., 2007);

the value of $\gamma_{A\text{- transcript}}$ half-life was set to equal the average of the half-lives of *AtARF3* and *AtARF4* transcripts (Narsai et al., 2007), and the effect of varying this parameter is extensively explored below; the value of $\gamma_{A\text{- transcript}}$ used to describe the *Ppsgs3* genotype in **Figure 4C, D** and **Figure 5A** was set to a value that results in a steady-state [$A\text{-}_{transcript}$] value ~2.5x higher than that in wild-type, which is consistent with experimental data on *PpARFb* expression in *Ppsgs3* (**Figure 2A**). Other parameter values are based on data from non-plant species (Vernoux et al., 2011). Importantly, the parameter space for such terms was also extensively explored, and found to not affect the outcomes of the model (see below).

A unique steady state exists for the auxin response GRN across a wide range of parameter values

Here, we demonstrate that a unique steady state equilibrium exists for the equations describing the behavior of the auxin response GRN across a wide range of parameter values. To this end, we expressed all equilibrium equations, i.e. when the left side of **Equations S1-S4** and **S6-S9** equals 0, in terms of [A+]. We then numerically solved for the steady state value of [A+], which showed that one and only one such value exists for the auxin response GRN for the parameter space described in **Table SM1**.

We first express [IA] in terms of [$D_{IA:A+}$] and [A+] by solving **Equations S2** and **S4** at steady state:

$$[\mathrm{IA}] = \frac{[\mathrm{D_{IA:A+}}] * (k'_{\mathrm{IX}} + \gamma_{\mathrm{IX}} + \gamma_{\mathrm{AUXIN}}(\mathrm{x}))}{k_{\mathrm{IX}} * [\mathrm{A+}]} \quad \text{(S10a)}$$

and

$$[\mathrm{IA}] = \frac{\pi_{\mathrm{A+}} + [\mathrm{D_{IA:A+}}] * (k'_{\mathrm{IX}} + * \gamma_{\mathrm{AUXIN}}(\mathrm{x})) - [\mathrm{A+}] * \gamma_{\mathrm{A+}}}{k_{\mathrm{IX}} * [\mathrm{A+}]} \quad \text{(S10b)}$$

eliminating [IA] from **S10a** and **S10b**:

$[\mathrm{D_{IA:A+}}] * (k'_{\mathrm{IX}} + \gamma_{\mathrm{IX}} + \gamma_{\mathrm{AUXIN}}(\mathrm{x})) = \pi_{\mathrm{A+}} + [\mathrm{D_{IA:A+}}] * (k'_{\mathrm{IX}} + * \gamma_{\mathrm{AUXIN}}(\mathrm{x})) - [\mathrm{A+}] * \gamma_{\mathrm{A+}}$, which allows [$D_{IA:A+}$] to be expressed as a function of [A+]:

$$\left[D_{IA:A+}\right] = \frac{\pi_{A+} - \left[A+\right] * \gamma_{A+}}{\gamma_{IX}} \quad \text{(S11)}$$

Equations S10a and **S11** allow [IA] to be expressed in terms of [A+]:

$$\left[IA\right] = \frac{k'_{IX} + \gamma_{IX} + \gamma_{AUXIN}(x)}{\gamma_{IX} * k_{IX}} \left(\frac{\pi_{A+}}{\left[A+\right]} - \gamma_{A+} \right) \quad \text{(S12)}$$

Abbreviating $Y(x) = k'_{IX} + \gamma_{IX} + \gamma_{AUXIN}(x)$, and solving **Equation S3** at steady state, we get $\left[D_{IA:IA}\right] = \frac{k_{IX} * \left[IA\right]^2}{Y(x)}$, which, by replacing [IA] with **Equation S12**, allows $[D_{IA:IA}]$ to be expressed in terms of [A+]:

$$\left[D_{IA:IA}\right] = \frac{Y(x)}{\gamma_{IX}^{\ 2} * k_{IX}} \left(\frac{\pi_{A+}}{\left[A+\right]} - \gamma_{A+} \right)^2 \quad \text{(S13)}$$

The steady-state level of [A-] (**Equation S6**) is linearly dependent on steady-state $[A\text{-}_{transcript}]$:

$$\left[A-\right] = \frac{\pi_{A-}}{\gamma_{A-}} * [A-_{TRANSCRIPT}] \quad \text{(S14)}$$

$[IA_{transcript}]$ and $[A\text{-}_{transcript}]$ are linearly dependent on ARG transcription rate, h (**Equations S7-S8**):

$$[IA_{TRANSCRIPT}] = \frac{h\left(\left[A+\right],[IA],\left[A-\right],\left[D_{IA:A+}\right]\right)}{2 * \gamma_{IA\ transcript}} \quad \text{(S15)}$$

$$[A-_{TRANSCRIPT}] = \frac{h\left(\left[A+\right],[IA],\left[A-\right],\left[D_{IA:A+}\right]\right)}{2 * \gamma_{A-\ transcript}} \quad \text{(S16)}$$

Equations S15 and **S16** allow [A-] to be expressed in terms of $[IA_{transcript}]$:

$$[A-_{TRANSCRIPT}] = \frac{\gamma_{IA\ transcript} * [IA_{TRANSCRIPT}]}{\gamma_{A-\ transcript}} \quad \text{(S16b)}$$

and therefore,

$$\left[A-\right] = \frac{\pi_{A-} * \gamma_{IA\ transcript} * [IA_{TRANSCRIPT}]}{\gamma_{A-} * \gamma_{A-\ transcript}} \quad \text{(S17)}$$

$[IA_{transcript}]$ can also be expressed in terms of [A+] by solving **Equation S1** at steady state:

$$-\pi_{IA} * [IA_{TRANSCRIPT}] = 2 * k'_{IX} * [D_{IA:IA}] - 2 * k_{IX} * [IA]^2 + k'_{IX} * [D_{IA:A+}] - k_{IX} * [IA] * [A+] + \ldots$$
$$[D_{IA:IA}] * \gamma_{AUXIN}(x) - [IA] * \gamma_{AUXIN}(x)$$

which, after substituting **Equations S11**, **S13**, as well as the steady-state solution of **Equation S3**, becomes:

$$[IA_{TRANSCRIPT}] = -\frac{1}{\pi_{IA}}\left(\frac{[IA]^2 * k_{IX}}{Y(x)} * \left(\gamma_{AUXIN}(x) + 2k'_{IX}\right) + [IA]\left(-2 * k_{IX} * [IA] - k_{IX} * [A+] - \ldots\right.\right.$$
$$\left.\left.\gamma_{AUXIN}(x)\right) + k'_{IX} * [D_{IA:A+}]\right)$$

This, after abbreviating $U = \left(\frac{\pi_{A+}}{[A+]} - \gamma_{A+}\right)$ and substitution of **Equation S12**, becomes:

$$[IA_{TRANSCRIPT}] = \frac{1}{\pi_{IA}}\left(\frac{U}{\gamma_{IX}}\left(\frac{U * \gamma_{AUXIN}(x)}{\gamma_{IX} * k_{IX}}\left(2 * \gamma_{IX} + \gamma_{AUXIN}(x)\right) + \left(\gamma_{IX} - \gamma_{AUXIN}(x)\right) * [A+] + \right.\right.$$
$$\left.\left.\frac{Y(x) * \gamma_{AUXIN}(x)}{k_{IX}}\right)\right), \text{ or}$$

$$[IA_{TRANSCRIPT}] = \frac{1}{\pi_{IA}}\left(\frac{\left(\frac{\pi_{A+}}{[A+]} - \gamma_{A+}\right)}{\gamma_{IX}}\left(\frac{\left(\frac{\pi_{A+}}{[A+]} - \gamma_{A+}\right) * \gamma_{AUXIN}(x)}{\gamma_{IX} * k_{IX}}\left(2 * \gamma_{IX} + \gamma_{AUXIN}(x)\right) + \ldots\right.\right. \quad \text{(S18)}$$
$$\left.\left.\left(\gamma_{IX} - \gamma_{AUXIN}(x)\right) * [A+] + \frac{Y(x) * \gamma_{AUXIN}(x)}{k_{IX}}\right)\right)$$

Finally, we substitute **Equations S9**, **S11, S12, S13, S17** into **Equation S7**:

$$\frac{d[IA_{TRANSCRIPT}]}{dt} = h\left([A+],[IA],[A-],[D_{IA:A+}]\right) - 2 * \gamma_{IA\ transcript} * [IA_{TRANSCRIPT}]$$

$$\frac{d[IA_{TRANSCRIPT}]}{dt} = \frac{1 + \frac{f * [A+]}{k'_P} * \left(1 + \frac{f_A * \omega_A * [A+]}{k'_P}\right)}{1 + \frac{[A+]}{k'_P} * \left(1 + \frac{\omega_A * [A+]}{k'_P}\right) + \frac{\omega_I * [A+] * [IA]}{K_{dIX} k'_P} + \frac{\omega_D * [D_{IA:A+}]}{k'_P} + \frac{[A-]}{k'_P}} - \ldots$$
$$2 * \gamma_{IA\ transcript} * [IA_{TRANSCRIPT}]$$

$$\frac{d[\mathrm{IA_{TRANSCRIPT}}]}{d\mathrm{t}} = \left(1 + \frac{f * [\mathrm{A+}]}{k'_{\mathrm{P}}} * \left(1 + \frac{f_{\mathrm{A}} * \omega_{\mathrm{A}} * [\mathrm{A+}]}{k'_{\mathrm{P}}}\right)\right) \Bigg/ \left(1 + \frac{[\mathrm{A+}]}{k'_{\mathrm{P}}} * \left(1 + \frac{\omega_{\mathrm{A}} * [\mathrm{A+}]}{k'_{\mathrm{P}}}\right) + \ldots \right.$$
$$\frac{\omega_{\mathrm{I}} * [\mathrm{A+}] * \mathrm{Y} * \left(\frac{\pi_{\mathrm{A+}}}{[\mathrm{A+}]} - \gamma_{\mathrm{A+}}\right)}{K_{\mathrm{dIX}} k'_{\mathrm{P}} * \gamma_{\mathrm{IX}} * k_{\mathrm{IX}}} + \frac{\omega_{\mathrm{D}} * \left(\pi_{\mathrm{A+}} - [\mathrm{A+}] * \gamma_{\mathrm{A+}}\right)}{k'_{\mathrm{P}} * \gamma_{\mathrm{IX}}} + \ldots$$
$$\left. \frac{\pi_{\mathrm{A-}} * \gamma_{\mathrm{IA\ transcript}} * [\mathrm{IA_{TRANSCRIPT}}]}{k'_{\mathrm{P}} * \gamma_{\mathrm{A-}} * \gamma_{\mathrm{A-\ transcript}}}\right) - 2 * \gamma_{\mathrm{IA\ transcript}} * [\mathrm{IA_{TRANSCRIPT}}] \qquad \text{(S19)}$$

By substituting **Equation S18** into **Equation S19**, we can define a function, $\frac{d[\mathrm{IA_{TRANSCRIPT}}]}{d\mathrm{t}}([\mathrm{A+}])$, such that the auxin response GRN is at equilibrium when $\frac{d[\mathrm{IA_{TRANSCRIPT}}]}{d\mathrm{t}}([\mathrm{A+}]) = 0$. This allows a solution for the equilibrium value of [A+]; however, it is apparent that this solution is not easily found analytically. Instead, to demonstrate that the system of equations describing the auxin response GRN is consistent with only one steady-state solution for [A+], we solved **Equation S19** numerically across possible values of [A+] and a wide range of parameter values. Because none of the variables representing molecular concentrations can be negative, **Equations S11, S12, S13, S16b, S17**, and S**18** allow us to define the range of possible equilibrium [A+] values. In order for [$D_{IA:A+}$], [$D_{IA:IA}$], and [IA] to be non-negative and defined, the steady-state concentration of [A+] must satisfy $0 < [\mathrm{A+}] \leq \frac{\pi_{\mathrm{A+}}}{\gamma_{\mathrm{A+}}}$. Since the range of acceptable [A+] values does not include 0, we used 10 fM as the lower bound value for [A+]: assuming a protonemal cell volume of ~200 picoliters, which we determined to be the volume of a typical protonema-derived protoplast, 10 fM represents ~1 molecule/cell. In order to identify values of [A+] that allow for non-negative, defined values of [$IA_{transcript}$], and thus of [$A-_{transcript}$] and [A-], we numerically solved **Equation S18** to identify all values of [A+] where [$IA_{transcript}$] ≥ 0. For all parameter sets tested, all steady-state values of [A+] in the interval $10\ \mathrm{fM} < [\mathrm{A+}] \leq \frac{\pi_{\mathrm{A+}}}{\gamma_{\mathrm{A+}}}$ result in positive, defined values of [$IA_{transcript}$].

To numerically determine whether multiple equilibrium states exist for the auxin response GRN across the set of parameters described in **Table SM1**, we evaluated **Equation S19** (with **Equation S18** substituted in for $[IA_{transcript}]$) across values of [A+] in the interval $10\ fM < [A+] \leq \frac{\pi_{A+}}{\gamma_{A+}}$. The number of times that the function $\frac{d[IA_{TRANSCRIPT}]}{dt}([A+]) = 0$ indicates the number of steady states of [A+] that exist for the auxin response GRN. In turn, all other auxin response GRN components have a single steady-state solution for every value of [A+]. Thus, a single steady-state solution of [A+] would imply a single steady-state equilibrium point for the whole auxin response GRN. **Figure SM2** shows that, for each set of parameter values tested, there is one and only one value of [A+] that satisfies **Equation S19** at steady state. Thus, although we cannot rule out that there exists a set of parameters for which the auxin response GRN is bistable, for a wide range of biologically relevant parameter values, there is only one set of steady-state solutions for the components of the auxin response GRN.

Measurements of susceptibility and noise amplification

Recall that susceptibility (also referred to as sensitivity or gain) is defined as change in output over change in input (Bintu et al., 2005b; Hornung and Barkai, 2008). Following Hornung and Barkai (2008), we measured susceptibility by perturbing input by 1% and measuring the corresponding change in output. In our case, input is auxin signaling input level, and output is ARG expression or specifically $[IA_{transcript}]$:

$$\text{susceptibility} = \frac{\left([IA_{TRANSCRIPT}]_1 - [IA_{TRANSCRIPT}]_0\right) / [IA_{TRANSCRIPT}]_0}{\left(Auxin_1 - Auxin_0\right) / Auxin_0}$$

In all cases except where otherwise specified, starting auxin levels ($Auxin_0$) were set to 3.11, which represents an intermediate auxin signaling level, and this value was increased by 1% for $Auxin_1$. To measure $[IA_{transcript}]_0$ and $[IA_{transcript}]_1$, the absolute value of **Equation S19** with $Auxin_0$ and $Auxin_1$ as parameters was first minimized using MATLAB in the interval $10\ fM < [A+] \leq \frac{\pi_{A+}}{\gamma_{A+}}$ to identify the steady-state value of [A+]. This value was then used in **Equation S18** to calculate the steady-state value of $[IA_{transcript}]$ at each auxin concentration.

Measurements of noise amplification were made by simulations of stochastic fluctuations in auxin signals, where the levels of GRN components at each time step (0.001 minutes) were deterministically dependent on the current auxin signaling level and the GRN component levels at the previous time step, as described in **Equations S1-S9**. First, steady-state values of all auxin response GRN components were determined for a given set of parameters (see **Table SM1** for the wild-type parameters used). Steady states were determined by identifying the steady state value of [A+] as above, and then using **Equations S11, S12, S13, S16b, S17,** and **S18** to identify the steady state values of the other GRN components. For the input, a string of auxin values 1000 min long was generated. Because there is currently insufficient experimental data to determine the properties of auxin signaling input noise in plants, we performed analyses across a wide range of auxin noise parameters, discussed below. As a primary analysis, a Gaussian distribution of auxin values with a standard deviation of 30% of the mean auxin value was used. This distribution was truncated at a basal auxin level of $x_{basal} = \frac{1}{K_{AUXIN} * (\gamma_{MAX} - 1)}$ to ensure that γ_{AUXIN} was never lower than the degradation rate of Aux/IAA in the absence of auxin, γ_{IA} (see Vernoux et al., 2011). Each auxin level persisted for a noise spike period of 30 minutes before auxin level was set to a different value drawn at random from the auxin distribution. The effect of altering the values of noise parameters is extensively explored below.

Noise amplification was measured by simulating the response to the sequence of auxin values generated as described above, starting the system at steady state levels. Noise amplification is the ratio between output and input noise, where noise is defined as the mean-normalized standard deviation in input or output levels (Hornung and Barkai, 2008):

$$\text{noise amplification} = \frac{\sigma\left(\left[IA_{TRANSCRIPT}\right]\right) / \left\langle\left[IA_{TRANSCRIPT}\right]\right\rangle}{\sigma(\text{Auxin}) / \langle\text{Auxin}\rangle}$$

For each simulation, we calculated the standard deviation and mean of the auxin input and $[IA_{transcript}]$ output. These were then used to compute a noise amplification value. 50 replicate simulations were performed for each parameter set, drawing a new set of auxin input values each time. This allowed us to calculate a mean and standard error for noise amplification for each set of parameters tested.

Effects of small RNA regulation on noise amplification and susceptibility is robust across a wide range of parameter values

An important consideration is the degree to which results are robust to alternate choices of parameter values, especially as a subset of parameter values used are inferred from non-plant species. In addition, parameter values may well vary depending on cell type or perhaps in response to environmental inputs. Furthermore, for the purpose of tractability, the model makes certain simplifications in that only one auxin-dependent promoter with a single pair of ARF binding sites is modeled, and that Aux/IAA, activator ARF, and repressor ARF factors are modeled as single genes rather than members of gene families that may possess different affinity, translation, and degradation parameters. Such simplifications are unlikely to affect the qualitative properties of the relationship between tasiARF activity and susceptibility or noise amplification explored here, but these can complicate the connection of *in vivo* measurements directly to specific parameter values. Calculations of susceptibility and noise amplification simulations were therefore repeated using a wide range of parameter values, varying one parameter at a time (**Figure SM3**). Under the starting set of parameter values reported in **Table SM1**, both susceptibility and noise amplification increase as $\gamma_{A\text{- transcript}}$ increases, until a critical $\gamma_{A\text{- transcript}}$ level is reached (**Figure 4E; Figure SM3**). At this point, susceptibility and noise amplification either level out or dip slightly before leveling out. Alternative parameter values resulted primarily in quantitative changes in noise amplification and susceptibility as a function of $\gamma_{A\text{-transcript}}$. Parameters related to auxin signaling input level affect the absolute level of susceptibility and noise amplification at high $\gamma_{A\text{- transcript}}$ values (**Figure SM3A-C, F, H-J, L**), whereas changing values for translation rate of repressors of the auxin response, Aux/IAA and repressor ARFs (π_I and $\pi_{A\text{-}}$), alters the values of $\gamma_{A\text{- transcript}}$ over which noise amplification or susceptibility increased most (**Figure SM3O, P**). Alternate values of parameters such as *f* and *fA*, which represent the strength of RNA polymerase recruitment by activator ARFs, and γ_A and γ_{IX}, the baseline degradation rates of Aux/IAA monomers and dimers, alter the steepness of the 'dip' that occurs at high $\gamma_{A\text{- transcript}}$ values after the initial rise in susceptibility and noise amplification levels (**Figure SM3E, I, J)**. However, the most important finding from this parameter exploration is that, except for the most extreme parameter values, the relationship between repressor ARF transcript degradation rate, susceptibility, and noise amplification remains

consistent. Thus, the prediction that small RNA regulation increases both susceptibility and amplification of extrinsic noise is robust to the values of the parameters used in this model of the auxin response GRN.

Effects of small RNA regulation on noise amplification and susceptibility is robust to auxin signaling input noise properties

Because the statistical properties of extrinsic auxin noise in plants remain largely unexplored, we further assayed the effect of changing the variance of auxin levels, as well as the 'noise spike period' or the length of time that a particular level of auxin lasts (**Figure SM4**). Since noise amplification is a relative measure of output noise to input noise, altering input noise levels would have no effect on output noise if a linear relationship between input and output noise exists. However, increasing input noise levels resulted in higher noise amplification (**Figure SM4A**), demonstrating that the relationship between auxin signaling noise and ARG expression noise is non-linear. We also found that increasing the 'noise spike period' results in increased noise amplification (**Figure SM4B**). This result is intuitive whenever time averaging by the GRN plays a role in buffering input noise. Longer periods of input signal that deviate from the mean level of input would allow the genetic network more time to adapt towards a new steady state, thus deviating output levels away from their mean expression value.

Finally, we tested the effect of drawing auxin values from a Poisson, rather than a Gaussian, distribution in which the mean (and thus also the variance) of auxin signaling input level was set to 3.11. The primary source of auxin signaling input noise is unknown, but if auxin noise *in vivo* is the result of independent, discrete stochastic bursts of auxin production or transport, a Poisson distribution may better reflect the distribution of auxin levels experienced by a cell than a Gaussian distribution would. We find that the initial increase of noise amplification over increasing $\gamma_{A\text{- transcript}}$ values is steeper if auxin signaling input noise is Poisson-distributed rather than Gaussian-distributed (**Figure SM4C**). However, the characteristic dip and leveling-off of noise amplification occur at similar $\gamma_{A\text{- transcript}}$ values regardless of the distribution from which auxin values are drawn. Thus, although changing auxin noise parameters affects the quantitative levels of noise amplification, we find that the qualitative effect of increasing $\gamma_{A\text{- transcript}}$ on noise amplification does not depend on the properties of the auxin noise distribution.

Small RNA regulation increases noise amplification and susceptibility regardless of the mechanism of repression

In the main text, we show that, if the effect of small RNA regulation is modeled as an increase in $\gamma_{A\text{- transcript}}$, lowering small RNA levels, as in *Ppsgs3*, results in an increase in both susceptibility and extrinsic auxin signaling noise amplification. However, in addition to promoting target transcript degradation, small RNAs can influence target translation rate (Jones-Rhoades et al., 2006). To computationally assay the effect of tasiRNA activity via translational repression, we modeled the effect of changes in $\pi_{A\text{-}}$ on susceptibility and noise amplification. We find that, consistent with our results from $\gamma_{A\text{- transcript}}$ modulation, a decrease in small RNA levels and thus an increase in $\pi_{A\text{-}}$ results in increased susceptibility and extrinsic noise amplification (**Figure SM5**).

Negative feedback between auxin signaling and repressor ARF expression reduces susceptibility without a significant change in extrinsic noise amplification

Our experimental data indicates that expression of tasiARF-regulated repressor ARF genes is induced in response to auxin signaling (**Figure 4A**), and this negative feedback loop was incorporated into the model (**Figure SM1**; **Equation S8**). Previous theoretical work has been equivocal regarding the effect of negative feedback on extrinsic noise amplification. Autorepression can either increase extrinsic noise amplification by decreasing time-averaging, or decrease noise amplification by decreasing susceptibility (Paulsson, 2004). We thus sought to computationally assay the effect of auxin-dependent regulation of repressor ARF genes on susceptibility and noise amplification in the auxin response. To model the auxin response GRN without negative feedback regulation from repressor ARF proteins, an auxin-independent model for $A\text{-}_{transcript}$ transcription is necessary. $A\text{-}_{transcript}$ transcription rate was therefore set to a constant value equal to that of $A\text{-}_{transcript}$ in the presence of feedback (**Equation S8**), as this allows for a direct comparison of the auxin response GRN output with and without feedback regulation. Thus, for a given set of parameters, steady-state values of all auxin GRN components, including the auxin GRN output, $[IA_{transcript}]_0$, are identical regardless of whether there is feedback. However, when auxin signaling input levels change, $[A\text{-}_{transcript}]$ adjusts in the presence of feedback but stays constant in its absence, leading to differences in auxin response GRN outputs.

We find that susceptibility is much lower in the presence of repressive feedback than in its absence (**Figure SM6**). This result is consistent with both theoretical predictions (Paulsson, 2004) and previous modeling of simpler GRNs (Hornung and Barkai, 2008), and reflects the increase in ARF repressor levels that follow an increase in auxin input levels, in turn lowering ARG output. This intuitive relationship is, however, complicated in the case of the auxin response GRN, by the existence of a second negative feedback loop between auxin signaling and Aux/IAAs. Our modeling results indicate that even in this complex network with multiple instances of repressive feedback, theoretical predictions regarding susceptibility are upheld.

Previous theoretical work further indicates that loss of susceptibility as a result of negative feedback is a tradeoff for increased robustness to intrinsic noise (Paulsson, 2004). Increased robustness to intrinsic noise is also seen for GRNs with multiple repressive feedback loops (Longo et al., 2013). However, our results indicate that in the case of extrinsic noise amplification, any gains in robustness due to negative feedback are modest, and much smaller in magnitude than the concomitant loss of susceptibility (**Figure SM6A**). In the presence of feedback regulation, only a small, non-significant ($p = 0.12$ at $\gamma_{A\text{- transcript}} = 0.0016$) decrease in noise amplification is observed. These qualitative effects of feedback on susceptibility and noise amplification are consistent across different auxin signaling input levels, although the loss of susceptibility in the presence of feedback is especially pronounced at low auxin concentrations (**Figure SM6C**).

As in *Physcomitrella*, the *Arabidopsis* tasiRNA target *ARF4* is upregulated in response to auxin signaling (Paponov et al., 2008), suggesting that the properties lent to the auxin response GRN by ARF autoregulation in moss may hold true in flowering plants as well.

Effect of auxin signaling input level on steady-state ARG expression in wild-type and *Ppsgs3*

The computational model of the auxin response GRN suggests that small RNA regulation of repressor ARFs promotes susceptibility of the auxin response. However, this change in susceptibility is a measure of small differences in gene expression in response to very subtle

auxin signaling changes. To understand the effect of tasiARF regulation on gene expression in plants grown across a wide range of constant auxin concentrations, we calculated steady-state [$IA_{transcript}$] as above, across a range of auxin signaling input values. As in the simulations shown in **Figure 4D, E**, we used $\gamma_{A\text{- transcript}} = 0.0016$ as the 'wild-type' repressor ARF degradation rate, and modeled *Ppsgs3* by decreasing $\gamma_{A\text{- transcript}}$ 3.5-fold. The latter results in a ~2.5-fold upregulation of steady-state ARF- levels, consistent with the observed change in *PpARFb4* levels in *Ppsgs3* (**Figure 2A**). To ensure that the model correctly represents experiments in which varying amounts of auxin are added to growth media, we modeled the effect of adding auxin to a baseline level, where basal auxin value, as above, is $x_{basal} = \frac{1}{K_{AUXIN} * (\gamma_{MAX} - 1)}$. This amount of 'auxin added', rather than the total amount of auxin, is represented on the x-axis in **Figure 5A** to allow comparison of the qualitative properties of the model to experimental qRT-PCR results. As in experimental data, we normalized [$IA_{transcript}$] levels of both 'wild-type' and '*Ppsgs3*' in the model by the wild-type [$IA_{transcript}$] value at basal auxin signaling input values. The response of the GRN to increasing auxin levels at both $\gamma_{A\text{- transcript}}$ levels follows a sigmoid curve, but with much higher levels of relative [$IA_{transcript}$] induction achieved for the higher, 'wild-type'-like $\gamma_{A\text{-transcript}}$ value (**Figure 5A**), reflecting our *in vivo* data (**Figure 5B-G**).

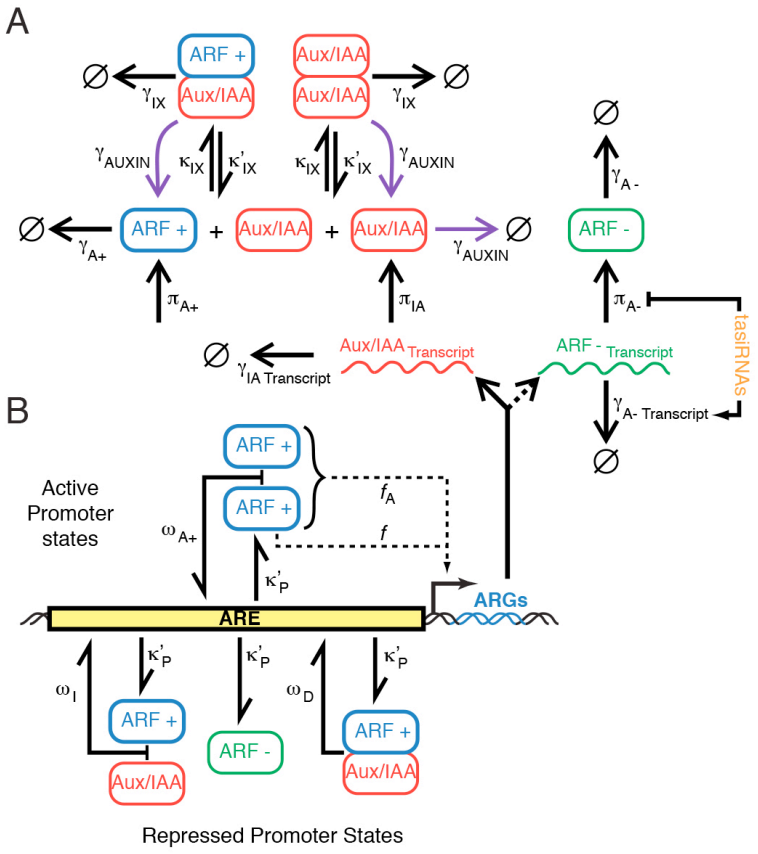

Figure SM1. Schematic of the computational model of the *Physcomitrella* auxin response network; for details on the parameters and ODEs governing the behavior of the model, see **Table SM1** and **Equations S1-S9**, respectively. (A) The model incorporates activator (ARF+) and repressor (ARF-) ARFs, as well as Aux/IAAs. Heterodimers between ARF+ and Aux/IAA, as well as Aux/IAA homodimers, can be degraded at a rate γ_{IX}. Both complexes associate and dissociate at rates κ_{IX} and κ'_{IX}, respectively. Furthermore, Aux/IAA either as a monomer or as part of a dimer is subject to auxin-dependent degradation, γ_{AUXIN}, which depends on an auxin signaling level, X, set in the model. ARF+ is produced at a constant rate π_{A+} and degraded at a rate γ_{A+}, whereas Aux/IAA is translated at a rate π_{IA} from available Aux/IAA transcript. ARF- is translated at a rate π_{A-} from available ARF- transcript, and degraded at a constant rate γ_{A-}. (B) Aux/IAA and ARF- transcripts are produced through the activity of a promoter controlled by an Auxin-Responsive Element (ARE). The ARE can bind any of the following with a dissociation constant κ'_P: ARF+ monomer or dimer (through cooperative promoter binding, with coefficient ω_{A+}) ; an ARF- monomer; a pre-formed ARF+/Aux/IAA heterodimer, which binds the promoter with cooperativity coefficient ω_D; or an ARF+/Aux/IAA heterodimer that forms on the promoter,

with a cooperativity coefficient ω_I. ARG transcription only occurs when the ARE in the promoter is bound by an ARF+ monomer or ARF+ dimer, which promote transcription with strength f or f_A, respectively. All other promoter-bound states, as well as the unbound state, are thus 'repressed'. The activity of the promoter governs the formation of Aux/IAA and ARF- transcript (the latter only when this negative feedback is included in the model). Aux/IAA transcript is degraded at a constant rate $\gamma_{IAtranscript}$, while ARF- transcript is degraded at rate $\gamma_{A\text{-}transcript}$. ARF- transcript degradation rate or translation rate can be increased or decreased, respectively, to simulate tasiRNA activity.

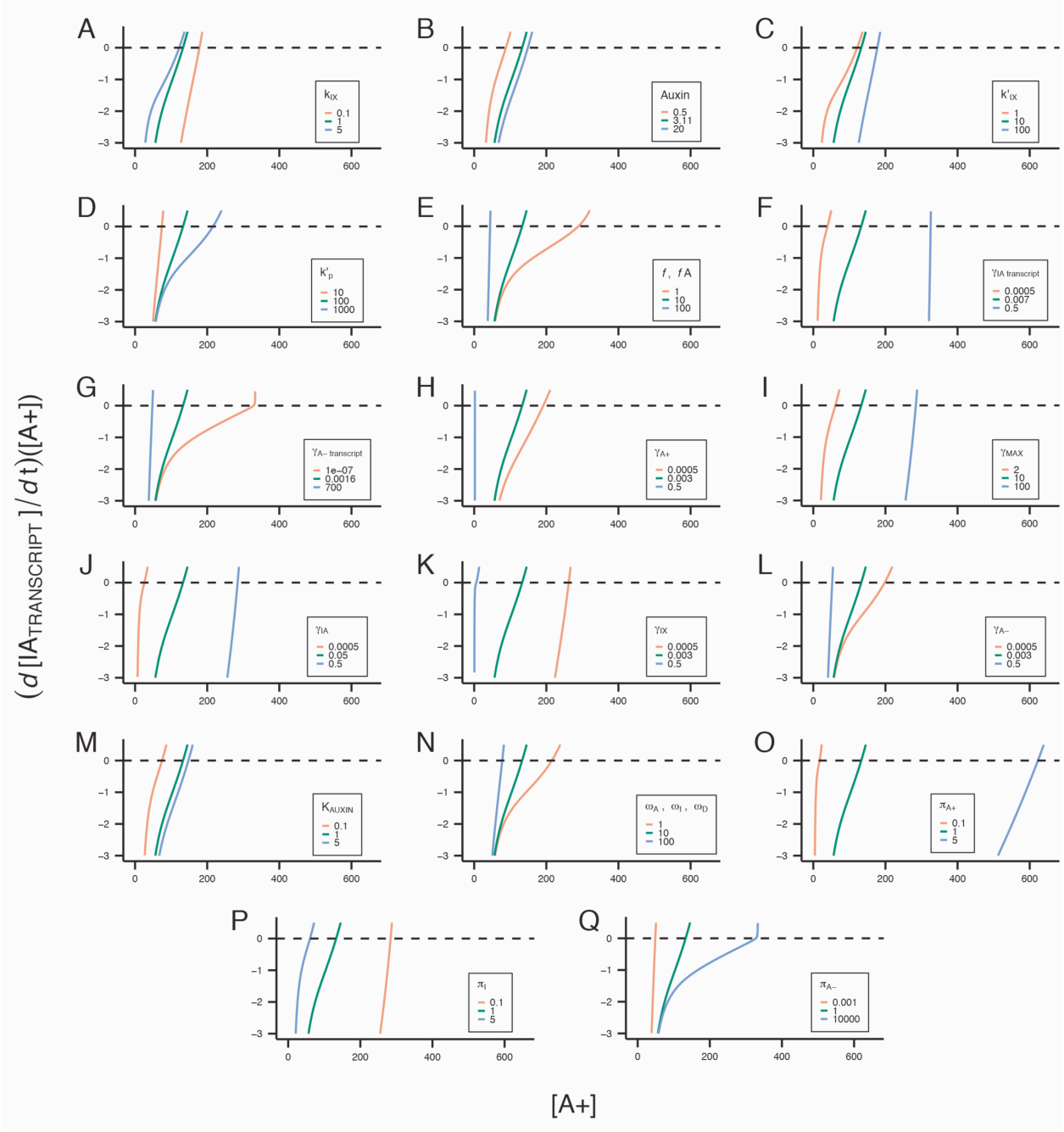

Figure SM2. Only one value of [A+] provides a steady-state solution for [$IA_{transcript}$]. Solutions to **Equation S19** for the range of possible [A+] values across a wide range of parameter values are shown. Note that the green line represents the same curve on all graphs, and is derived using the set of parameter values listed in 'Value in model' column of **Table SM1**.

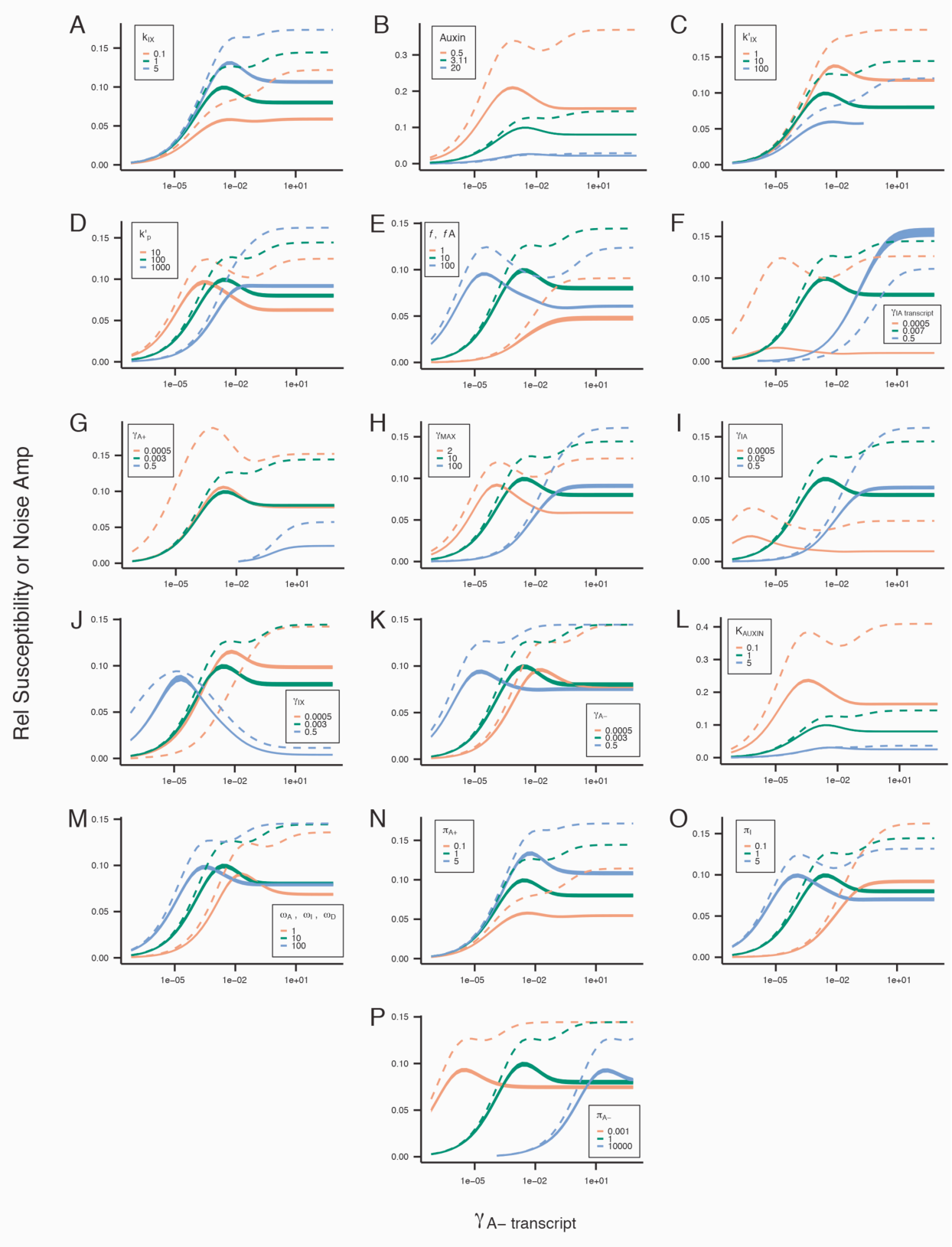
A
B
C
D
E
F
G
H
I
J
K
L
M
N
O
P
Rel Susceptibility or Noise Amp
γ A– transcript
1e−05
1e−02
1e+01
0.00
0.05
0.10
0.15
0.2
0.3
0.4
k_IX
0.1
1
5
Auxin
0.5
3.11
20
k'_IX
1
10
100
k'_p
10
100
1000
f , fA
1
10
100
γ_IA transcript
0.0005
0.007
0.5
γ_A+
0.0005
0.003
0.5
γ_MAX
2
10
100
γ_IA
0.0005
0.05
0.5
γ_IX
0.0005
0.003
0.5
γ_A–
0.0005
0.003
0.5
K_AUXIN
0.1
1
5
ω_A , ω_I , ω_D
1
10
100
π_A+
0.1
1
5
π_I
0.1
1
5
π_A–
0.001
1
10000

Figure SM3. Noise amplification and susceptibility follow largely the same pattern as $\gamma_{A\text{- transcript}}$ increases across a wide range of parameters. Values of noise amplification +/- SE (solid line with shading) and susceptibility (dotted line) of the auxin response GRN, with changes to values of every parameter used in the model. Note that the green line represents the same curve on all graphs, and is derived using the set of parameter values listed in 'Value in model' column of **Table SM1**.

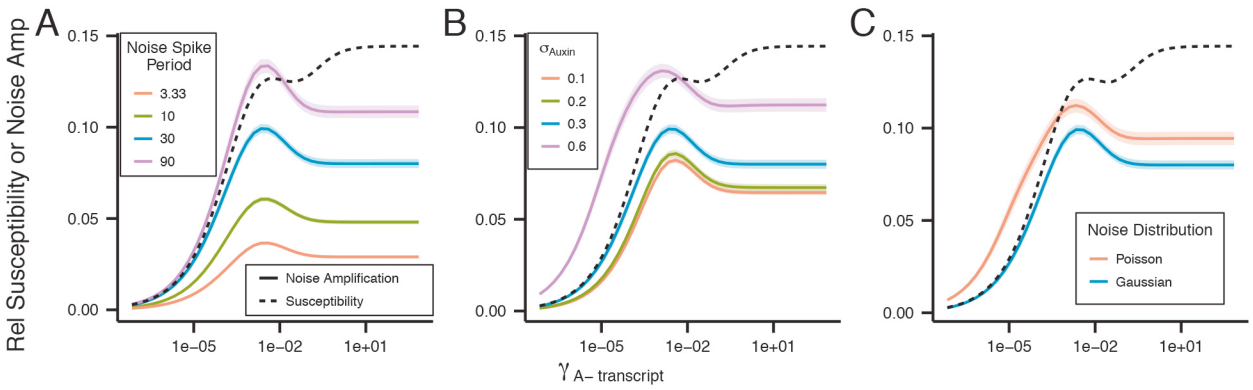

Figure SM4. Relationship between $\gamma_{A\text{- transcript}}$ and noise amplification holds over a wide range of auxin noise parameters. (A) Increasing periods of consistent auxin levels in a noisy input from ~3.3 minutes to ~90 minutes, increases the magnitude of noise amplification. (B) Increasing the standard deviation of auxin levels from 0.1*mean auxin level to 0.6*mean auxin level, increases the magnitude of noise amplification. (C) Modeling auxin noise as a Poisson distribution rather than a Gaussian distribution results in a steep increase in noise amplification at lower $\gamma_{A\text{- transcript}}$ values, but otherwise preserves the shape of the noise amplification curve.

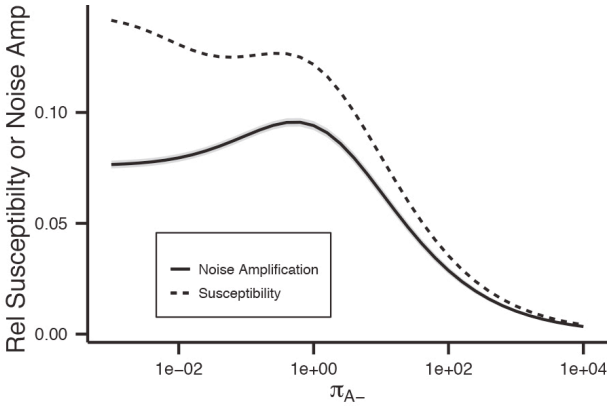

Figure SM5. Relationships between noise amplification or susceptibility and small RNA levels are independent of the mechanism of small RNA-mediated repression. The effect of modeling small RNA activity as a change in repressor ARF translation on susceptibility and noise amplification. Note that the graph resembles that shown in **Figure 4E**, but is reversed along the x-axis; while small RNA regulation increases $\gamma_{A\text{- transcript}}$, this decreases π_{A-}. Thus, increasing small RNA levels is plotted from right to left in this figure, but from left to right in **Figure 4E.**

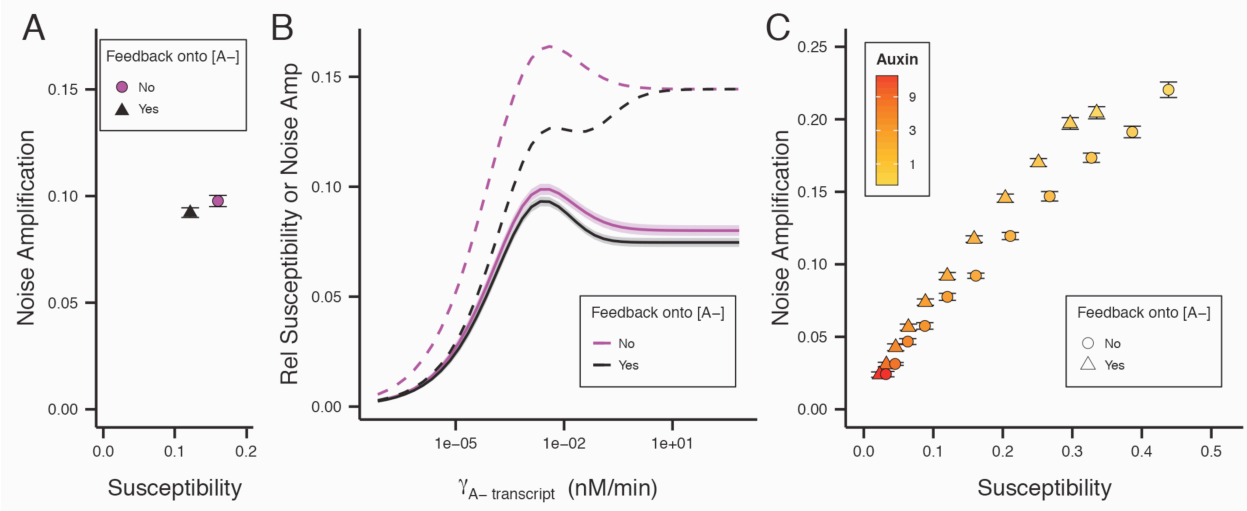

Figure SM6. Auxin signaling-mediated feedback onto repressor ARF genes strongly decreases susceptibility with little effect on extrinsic noise amplification. (A) Susceptibility (x-axis) and noise amplification +/- SE (y-axis) with and without negative autoregulation by repressor ARFs at $\gamma_{A\text{- transcript}} = 0.0016$ and Auxin = 3.11 shows that negative feedback results in a significant 24% decrease in susceptibility, and a non-significant 6% decrease in noise amplification ($p = 0.12$). (B) Differences in susceptibility and noise amplification between the auxin response GRN with and without feedback across a range of $\gamma_{A\text{- transcript}}$ values shows that negative feedback results in a consistent large decrease in susceptibility. Note that auxin input noise simulation at different $\gamma_{A\text{- transcript}}$ values is not independent. (C) Differences in susceptibility and noise amplification between the auxin response GRN with and without feedback across a range of Auxin values shows that feedback onto repressor ARF levels consistently results in a large decrease in susceptibility, but not in a consistent change in noise amplification.

REFERENCES

Bintu, L., Buchler, N.E., Garcia, H.G., Gerland, U., Hwa, T., Kondev, J., and Phillips, R. (2005a). Transcriptional regulation by the numbers: models. Curr Opin Genet Dev *15*, 116-124.

Bintu, L., Buchler, N.E., Garcia, H.G., Gerland, U., Hwa, T., Kondev, J., Kuhlman, T., and Phillips, R. (2005b). Transcriptional regulation by the numbers: applications. Curr Opin Genet Dev *15*, 125-135.

Hornung, G., and Barkai, N. (2008). Noise propagation and signaling sensitivity in biological networks: a role for positive feedback. PLoS Comput Biol *4*, e8.

Jones-Rhoades, M.W., Bartel, D.P., and Bartel, B. (2006). MicroRNAS and their regulatory roles in plants. Ann Rev Plant Biol *57*, 19-53.

Longo, D. M., Selimkhanov, J., Kearns, J. D., Hasty, J., Hoffmann, A., & Tsimring, L. S. (2013). Dual Delayed Feedback Provides Sensitivity and Robustness to the NF-κ B Signaling Module. PLoS Comput Biol *9*, e1003112.

Narsai, R., Howell, K.A., Millar, A.H., O'Toole, N., Small, I., and Whelan, J. (2007). Genome-wide analysis of mRNA decay rates and their determinants in Arabidopsis thaliana. Plant Cell *19*, 3418-3436.

Paulsson, J. (2004). Summing up the noise in gene networks. Nature *427*, 415-418.

Salmon, J., Ramos, J., and Callis, J. (2008). Degradation of the auxin response factor ARF1. Plant J *54*, 118-128.

Vernoux, T., Brunoud, G., Farcot, E., Morin, V., Van den Daele, H., Legrand, J., Oliva, M., Das, P., Larrieu, A., Wells, D., et al. (2011). The auxin signalling network translates dynamic input into robust patterning at the shoot apex. Mol Syst Biol *7*, 508.